Enlarged atomic force microscopy scanning scope: Novel sample-holder device with millimeter range

Ahmad Sinno, Pascal Ruaux, Luc Chassagne, Suat Topsu, Yasser Alayli, Gilles Lerondel, Sylvain Blaize, Aurélien Bruyant, Pascal Royer

Enlarged atomic force microscopy scanning scope: Novel sample-holder device with millimeter range

A. Sinno, P. Ruaux, L. Chassagne, S. Topçu, and Y. Alayli
LISV, University of Versailles, 45 Avenue des Etats Unis, 78035 Versailles, France

G. Lerondel, S. Blaize, A. Bruyant, and P. Royer
Laboratoire d'Instrumentation Optique et de Nanotechnologies, ICD, CNRS FRE 2848, Université de Technologie de Troyes, 12 Rue Marie Curie BP2060, 10010 Troyes, France

(Received 15 May 2007; accepted 29 July 2007; published online 27 September 2007)

We propose a homemade sample-holder unit used for nanopositionning in two dimensions with a millimeter traveling range. For each displacement axis, the system includes a long range traveling stage and a piezoelectric actuator for accurate positioning. Specific electronics is integrated according to metrological considerations, enhancing the repeatability performances. The aim of this work is to demonstrate that near-field microscopy at the scale of a chip is possible. For this we chose to characterize highly integrated optical structures. For this purpose, the sample holder was integrated into an atomic force microscope. A millimeter scale topographical image demonstrates the overall performances of the combined system. © *2007 American Institute of Physics.*
[DOI: 10.1063/1.2773623]

I. INTRODUCTION

With the development of nanotechnologies, scanning over large areas with a nanometer resolution is becoming more and more important. However, millimeter range scanning is not yet commercially available. This is because nanometer specifications such as resolution, positioning accuracy, and repeatability of the displacements are to meet all along the surface to cover. At the present time, with commercial systems, displacement is either limited to about a hundred of micrometers or possible on the millimeter scale but with limited accuracy and repeatability (typically in the order of the micrometers). Furthermore, repeatability is often neglected restricting the scope of applications. The technological progress of industrial apparatus makes us think this will be a serious challenge in the near future.[1] Yet, cutting-edge technologies are seeking new frontiers: microelectronics, near-field characterization of large scale structures, and electronic lithography for very large scale patterning, for example. The concepts of traceability, accuracy, and repeatability are thus essential. In this work, we report on a displacement system with a millimeter range and a nanometric positioning repeatability and traceability in both X and Y directions. In addition we show that this system is compatible with a commercially available atomic force microscopy (AFM) head.

This study was initially targeted toward applications in scanning probe microscopy (SPM). Surface inspection of optical components will require millimeter long scans along the light propagation axis. This is the case of lightwave device characterization where a combined AFM for topography imaging and a scanning near-field optical microscope (SNOM) for optical inspection is used. The aim is to observe the emitting or internal field of a structure according to its geometry.[2] Such a scan may reveal relevant information such as the phase and amplitude of the profiles of the guided field and from there, the mode effective indexes or refractive index profiles and local diffraction losses. When combined with Fourier transform, long scans become necessary to increase the precision of the refractive index measurement.[3] At the time being, SPM scans are only possible over 100 μm, which is the piezoelectric actuator (PZT) limit. Moreover, the electronic bandwidth of the PZT is quite low in these apparatus. The resolution is also limited by the acquisition system, which limits the number of points to typically 1024 in both directions. In this case, scanning over the full range of 100 μm leads to a poor resolution of about 100 nm. Nanometric resolution can thus be obtained only for micrometric scans.

The method currently used to overcome the 100 μm limit consists in stitching together overlapping elementary microscopic 2D scans.[3] A typical overlapping percentage of about 30% on each side of the scanned area is necessary. The overlapping scans are afterwards glued together by means of image processing techniques based on the localization of distinguishable topography patterns or defects that would match on the overlapping area. This process is time consuming and limited to the presence of a significant number of signatures on the surface that would allow a precise matching. For these reasons, this method is rarely used. Another solution is to use an array of probes. In Ref. 4, an image of 2×2 mm^2 was obtained but with a pixel size of 400 nm. This method requires to synchronously acquire the data from each probe, in addition to precisely mount the array of probes.

For positioning over millimeter ranges with high resolutions, the solution which appeared recently is the coupling of a mechanical displacement stage for long range motion with a precision stage for accurate positioning.[5–7] Still under development for years to come, several metrology institutes in the world have launched projects of sample-holder systems

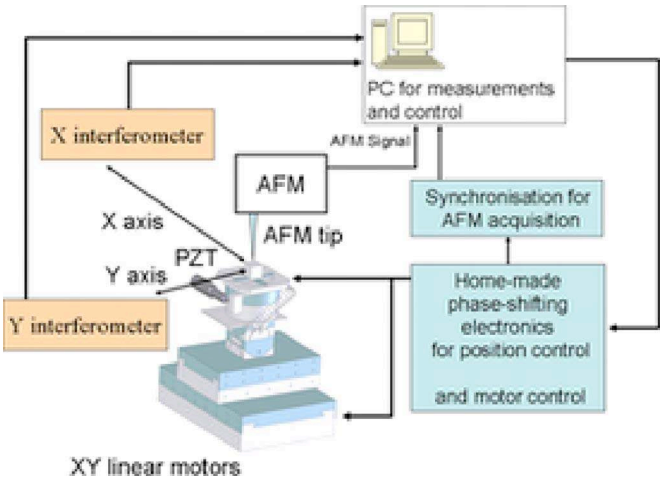

FIG. 1. (Color online) Sketch of the system. The double mechanical stage is composed of the *XY* linear motors and an *XY* piezoelectric actuator. Two interferometers allow real time position monitoring. The Personal computer (PC) unit controls the linear motors and the homemade electronic board that generates the phase-shift commands to control the piezoelectric actuators. AFM acquisition is synchronized with the *XY* displacements.

with nanometric resolution and accuracy over millimeter ranges: NIST (National Institute of Standards and Technology) in the USA,[8,9] PTB (Physikalisch-Technische Bundesanstalt) in Germany,[10] Metas in Switzerland,[11] NPL (National Physic Laboratory) in the United Kingdom,[12,13] NIM (National Institute of Metrology) in China, and LNE (Laboratoire National de métrologie et d'Essais) in France.[14] Furthermore, many works were initiated to develop an apparatus usually named metrological atomic force microscope[15–21] (MAFM), but most of them still present some limitations with the traceability and the reproducibility of the imaging process; hysteresis and nonlinearity defects of the piezoelectric actuator induce problems of repeatability of the motion. It seems very difficult to cross the 100 nm barrier in accuracy without compensation.[22] First, apparatus integrating these capabilities are being developed in laboratories. A first demonstration of a long scan was illustrated in Ref. 10, but with a resolution of only 100 nm and a very long time consumption budget where 12 h were necessary for a scan of 1 mm$\times$100 μm.

This article presents the system we proposed for precision scanning over millimeter range with high resolution. It is divided into two main sections. The first one is devoted to the scanning stage where after presenting the stage, hysteris, mechanical, software and scanning methods issues are addressed. In the second section, imaging results are presented. The overall performances of the combined system are finally discussed.

II. EXPERIMENTAL SETUP

A. Sketch of the system

In previous works, we presented an optoelectronic system able to perform displacement steps over millimeter ranges with nanometric accuracy and repeatability.[23] In this article, we extend the principle to a double axes system (Fig. 1). This system includes a double moving stage for each displacement axis. The first stage is a commercially available long range linear motor (Aerotech ANT-50) capable to move over 50 mm with a 10 nm resolution and a straightness of about 1 μm. The second stage comprising a piezoelectric actuator (PiezoSystem Jena) overcomes the defects of the first stage thanks to its subnanometric resolution and high bandwidth. Its full range is 15 μm but a low voltage amplifier limits its range to 3 μm. Position measurements are made with a frequency stabilized HeNe laser that ensures traceability and a double two-pass Michelson interferometer with a resolution of 0.31 nm. Such interferometers have a nonlinearity of 2 nm if finely adjusted.[24] A homemade high frequency electronic board equipped with a phase-shifting electronic (PSE) circuit acts as the core of the system.[25] It generates high frequency signals used as reference signals to synchronize the laser head and its measurement boards, the Zygo ZMI2001 boards. The PSE circuit controls the PZT actuators with subnanometric position steps by imposing well calibrated phase shifts between the reference signal and the measured signals. The performances of the electronic board in terms of positioning resolution and repeatability are at the nanometer scale. The phase shifts $\Delta\phi$ are configurable so that downscaled position steps Δd can be achieved according to the equation

$$\Delta d = \frac{\lambda_0 \Delta\phi}{8\pi n}, \tag{1}$$

where λ_0 is the wavelength of the laser source in vacuum and n the refractive index of air. The laser source was calibrated at the LNE. Its wavelength is equal to λ_0=632.991 528 nm with a relative uncertainty of 1.6×10^{-9} (1σ). The displacement resolution can be programed down to 0.25 nm. This phase-shifting principle frees our displacements from the nonlinearity and hysteresis effects of the PZT actuator. Detailed description of the HF board can be found in Ref. 25. A Zerodur® mirror cube acting as a moving mirror for the laser interferometers is placed on top of the *XY* PZT actuator and serves us to carry a sample on its top face, making of our system a sample-holder unit (SHU). The SHU is adapted under an atomic force microscope (M5 Park Scientific Instruments) allowing sample surface inspection beyond the microscope's area coverage limit. The SHU ensures the *XY* displacements, whereas the AFM controller handles the z-axis movements and the atomic force feedback. The z actuator of the microscope is a 7 μm range PZT scanner. The tip of the microscope is brought in close proximity of the sample surface. The tip-to-surface distance is controlled by the atomic force regulation. The whole system is supervised and controlled through a LABVIEW interface. The sketch of the system is presented in Fig. 2 on the upper part and a photography on the lower part.

B. Hysteresis control

In classical AFM controllers, intrinsic nonlinearity defects of the PZT-driven scanner are software controlled. The inverse hysteresis model is usually used[10,26] according to the equation

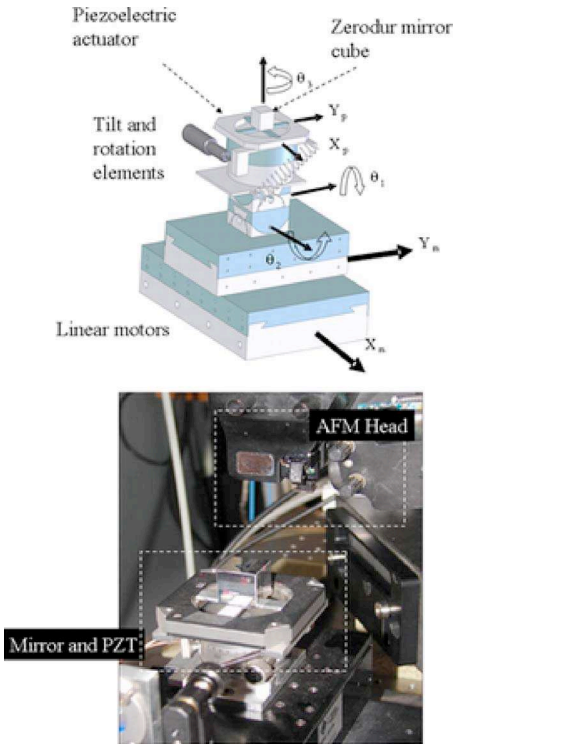

FIG. 2. (Color online) Top part: sketch and photography of the system. One can see the mirror cube where the sample is to be placed, the 2D piezoelectric actuator, the mechanical stages used for fine angles adjustments, the linear motors in addition to the AFM head on top of the displacement system. Tuning axes and angles are pointed out on the CAD design. (X_o, Y_o) optical axes, (X_P, Y_P) piezoelectric actuator axes, and (X_m, Y_m) linear motors axes must all be aligned previous to operation. Bottom part: photography of the AFM tip placed over the SHU.

$$V(x) = x^{-1}(V_0, x_0) \tag{2}$$

in order to calculate the desired control voltage V to apply to the PZT actuators to attain a position x as a function of the actual state (voltage V_0 and position x_0) of the actuator. This method presents two major drawbacks. The first one is that this equation encloses linearization coefficients that were defined under specific environmental conditions and implemented on board of the AFM controller. These coefficients and model will no more be valid if the conditions change and the PZT behavior will consequently not be the same. PZT actuators undergo aging with time and have a different behavior at each stable operating temperature. This makes the AFM displacements inaccurate, unless real time calibration is used. The SHU follows a different directive. The PZT in our system tries to keep track of the desired trajectory by locking the phase of the measured signal on the phase of the reference signal. This means that the PZT will contract/retract by the necessary distance until phase difference nulls, whatever the actual state of the PZT is and whatever the operating temperature at which the system has stabilized. Hysteresis, creep, and temporal instabilities of the PZT are eliminated which enhances the repeatability of the displacements. The second drawback is that Eq. (2) is usually software implemented in the AFM controller. Such equation usually incorporates a lot of coefficients and thus needs complex computation, especially when complex algorithms are used to better track the linear model.[27] This may have an annoying effect on the bandwidth of the control loop. In our system, nonlinearity rectification is hardware implemented based on the phase locking principle and depends on the robustness of the analog servo loop controller that is implemented.

C. Mechanical adjustments

Since the SHU operates over millimeter ranges, tiny mechanical defects are magnified and may become uncontrollable. Preliminary alignments are thus necessary to minimize errors before operating the SHU. The orthogonality between two perpendicular faces of the mirror cube is certified to be less than 1 arc sec. The orthogonality between the two linear motors was controlled using interferometry with an accuracy of 5 arc sec. Furthermore, several rotational stages inserted between the linear motors and the piezoelectric actuators allow angles and axes tuning (Fig. 2). The optical axes of the interferometers (X_o, Y_o), the mechanical axes of the linear motors (X_m, Y_m), and the mechanical axes of the piezoelectric actuators (X_p, Y_p) are finely aligned with an uncertainty lower than 5 arc sec.[28] The remaining straightness defects can be compensated by the piezoelectric action using the electronic feedback lock-in system. The sample to investigate is centered on the top face of the mirror cube and thus practically on the intersection point of X_o and Y_o for an Abbe error-free configuration. Another error to overcome when dealing with millimeter ranges is the tilt that may arise between the XY plane of the moving stages and that of the sample being scanned. The greater the tilt and the longer the distance covered, the more the PZT actuator of the microscope will have to contract/retract in the z direction in order to track the surface of the sample. A microscope equipped with a 10 μm range PZT actuator in the z axis will unlock after traveling 1 mm in the XY plane if a tilt of 10 mrad exists. This tilt causes an artifact giving the impression that the two sample surfaces are not parallel to each other. As far as mechanical vibrations are concerned, the interferometers, mechanical stages, and AFM apparatus lay on an active antivibration table that eliminates external noise. Temperature of the room is controlled in order to prevent any drift on the laser measurements[29] and mechanical parts.

D. Software adaptation and acquisition

AFM controllers present many limitations. With classical AFM software, the scans are programable with two major dimensional parameters: the size of the scan (in micrometers) and the number of points to sample for each line. This directly induces the spatial resolution of the image. The maximal number of points per line is usually limited to 1024. For example, a scan of 100×100 μm^2 displayed using 1024×1024 pixels leads to a resolution of about 100 nm in each direction. A scan of 1 mm long with 1024 sampled points would lead to a resolution of 1 μm/pixel. For this reason, we shunt the acquisition module of the AFM and take hand over it in order to increase the resolution especially for long range scans. A motion synchronized pulse firing controller (MSPFC) triggers the acquisition from the AFM synchronously with the SHU movements. The MSPFC pulses are derived from the signals of the optical encoders of the linear

motors and from the homemade phase-shifting board. Each time the SHU steps in the *XY* plane, the MSPFC launches an interrupt pulse toward a LABVIEW real time based data acquisition card that will acquire the *z*-position signal from the AFM. The analog to digital converter (ADC) of the acquisition board is a 16 bit converter and operates at sampling frequencies over 100 kHz. The MSPFC is able to output pulses which allow us to ally high speeds with high resolutions without altering the accuracy. The number of data points per line acquired is then only limited by the time resolution of the pulse incoming from the MSPFC synchronization board. The real limitation is, in fact, a software problem: the file system of the operating shell does not allow huge file indexation. For this, the acquisition software stores each set of lines in a file. A powerful computer able to handle the high speed flow of data when the SHU runs at high speeds and to process the resulting amount of data points is also needed. Furthermore, classical AFM softwares display the scanned surface in real time. This dramatically decreases the bandwidth of the acquisition since image nonlinearity corrections, among others, are processed online. Furthermore, the link between the AFM controller and the host computer used for display is usually an Ethernet connection[30] with a limited bandwidth that is not suitable for real time display of high speed data. In our system, data processing and displaying are made afterwards in order to visualize the three-dimensional (3D) topography image. The method we use produces data files containing the entire information, and any image processing script can be applied to reveal information about the sample such as artifact elimination or outlining specific features of the topography.

E. Scanning methods

Traditional AFM tips scan the surface of a sample in a zigzag trajectory mode by applying sweeping command signals on the piezoelectric actuators. A sweep is made to scan a line along the *X* axis, and a second slower sweep is made along the *Y* axis to compose the multiline profile. The SHU operates in a different manner. The *XY* controllers of the AFM are unused since the SHU is ensuring the *XY* displacements. The tip of the microscope is equipped with a PZT actuator that is acting only in the *z* direction. We then figured out three functional modes with different scanning strategies in order to move the sample relative to the tip over the millimeter range.

In the first mode, named "matrix by matrix" (MM mode), a multitude of elementary micrometric scans called matrices is achieved and jointed to compose the whole image—the mother matrix. An initialization phase is first made to mark a (0; 0) position in the $(X;Y)$ reference. Then a first elementary matrix is scanned by the piezoelectric actuators on micrometric range with preprogramed parameters such as speed, elementary area, and resolution. Elementary matrix area is limited to 3×3 μm^2 since achieved using the PZT actuators only. Once this first scan is achieved, the PZT actuators which attained their stretching limit are released. The linear motors then move on to displace the sample and position it in a way a new elementary matrix can be scanned accurately next to the previous one. The piezoelectric actuators can hence achieve several scans that are perfectly adjacent until an image composed of several elementary matrices is formed. Under MSPFC control, the acquisition points are synchronized with the phase-shifting system which ensures to be insensitive to the nonlinearities and defects of the piezoelectric actuators. The MSPFC launches an interrupt toward the AFM each time the PZT steps inside an elementary matrix. This mode resembles to the stitching process but no stitching is applied *a posteriori*. The phase-shifting positioning system ensures the accuracy of the connections between the elementary matrices; overlapping windows are not needed. The position uncertainty is programable, depending on the resolution of the positioning system which can be as low as 0.25 nm.[25] This mode is sufficiently accurate but its problem is that it is time consuming.

In the second mode, named "line per line" (LL mode), long lines are performed with the linear motors without piezoelectric compensation along the displacement axis. Only the straightness of the moving motor is controlled. The same initialization phase is made fixing a (0;0) position in the $(X;Y)$ reference. Then, a long line is directly performed by the linear motor along the *X* axis. The piezoelectric stage only compensates the straightness along the *Y* axis, but not the accuracy position defects along the *X* axis. When a line is done, the phase-shifting system repositions the sample for a second line strictly parallel to the previous one. This routine is applied until covering the whole area to scan. The resulting image is then accurate in the *Y* dimension. The length of the lines and the spacing between two lines are programable. The displacement resolution along the *X* axis is 10 nm since the linear motor is traveling alone without the help of the PZT stage. The MSPFC synchronizes the AFM acquisitions with the displacements of the linear motor. This mode is not optimized for position control but allows long scans easily and quickly. Speeds at the mm/s scale can be reached.

In the third mode, called "tracking trajectory mode" (TT mode), long lines are performed using the linear motors with real time piezoelectric compensation permanently activated on both axes. The linear motors and the PZT actuators cooperate together to travel long lines accurately. Each time the linear motor moves a step, the PZT actuator compensates its defects ensuring the positioning accuracy. This implies lower speeds. In fact, the PZT actuators have an open loop bandwidth of 2.5 kHz, but the closed loop control and the voltage amplifier scale it down to less than 1 kHz. Tests showed that a speed of 10 $\mu m/s$ is the maximum value so that the PZT actuators can track. At the end of each line, the PZT actuators will have contracted/retracted by the amount of nonlinearities, straightness, hysteresis, and other intrinsic defects of the system that were cumulated all along a line. The same outcomes are then inherited from the LL mode: straight and accurately distanced long lines, but in addition to this, intrinsic defects of the linear motors are compensated at each point. The TT mode is the ultimate mode since accurate in both dimensions but lacks of speed in addition to being the most difficult to optimize for all the lock-in loops involved in this type of mode control.

III. MEASUREMENTS AND DISCUSSIONS

A. Parameters of the experiment

The sample investigated is a silicon-on-insulator (SOI) substrate with a waveguide structures pattern. The waveguides are parallel but irregularly set. Their width is about 2.8 μm and their height around 160 nm. In order to minimize the total scanning time, the speed of the scan has to be maximized. For this purpose, the LL mode is the most convenient. A speed of 40 μm s^{-1} was chosen. The SHU allows higher speeds but this upper limit is fixed by the AFM operation regulations: damage may, in fact, be caused to the AFM tip if this speed is larger. The AFM is functioning in tapping mode. This implies that the signal that represents the surface profile is the voltage applied to the z-PZT actuator to keep constant the distance from the sample and null the error signal of the AFM control loop. It is this signal that is sent to the LABVIEW acquisition card for sampling, triggered externally with the pulses coming from the MSPFC that are synchronous with the long axis displacements. For a scan of 1 mm long, each line takes 25 s, but the positioning process at nanometric accuracy when the SHU is changing the line can be time consuming and takes around 30 s, so the total time for a line scan is around 1 min.

The image presented in Fig. 3 is 750 nm width (X axis) and 1 mm long (Y axis). The resolutions are 25 nm for the X axis (29 lines) and 20 nm for the Y axis. So there is 50 000 points per line along the Y axis. This is not limited by the apparatus or by the acquisition system, but we preferred to limit the number of points to make the data treatment easier. The Z axis represents the AFM topography signal.

B. Results for long topography imaging

Figure 3 was obtained using MATLAB software. The upper part of the figure is presented without any post-treatment (raw image). Note that the long scan axis is Y, whereas X stands for the short scan direction. We can notice shading off of colors in the image because of the remaining tilts in X and Y axes. Due to the data high density, the image is not really easy to read. One can see the parallel waveguide structures along the X axis and their irregular layout. The lower part shows the same image but after background correction. Here, the background is mainly due to a residual tilt between the sample and the top face of the cube and a thermal drift during the acquisition process. A thermal drift acts to expand the metrological chain of the system. This chain includes the body of the microscope in addition to the multistacked elements of the SHU.

In order to analyze the data along the long scan axis Y, a cross section is pointed out in Fig. 4. The upper part is presented, also without any post-treatment (raw profile). The waveguide structures clearly appear here. They seem to be distorted, but it is only an artifact due to the disproportional representation of high density data on the Y axis with respect to the X axis. This cross section was flattened using a third order polynomial fit and is shown in the lower part of the figure. The equation used for the background correction is $Z=-390+1.96Y-7.67\times10^{-7}Y^2+3.3\times10^{-13}Y^3$, where Y is expressed in micrometers. This correction may have several

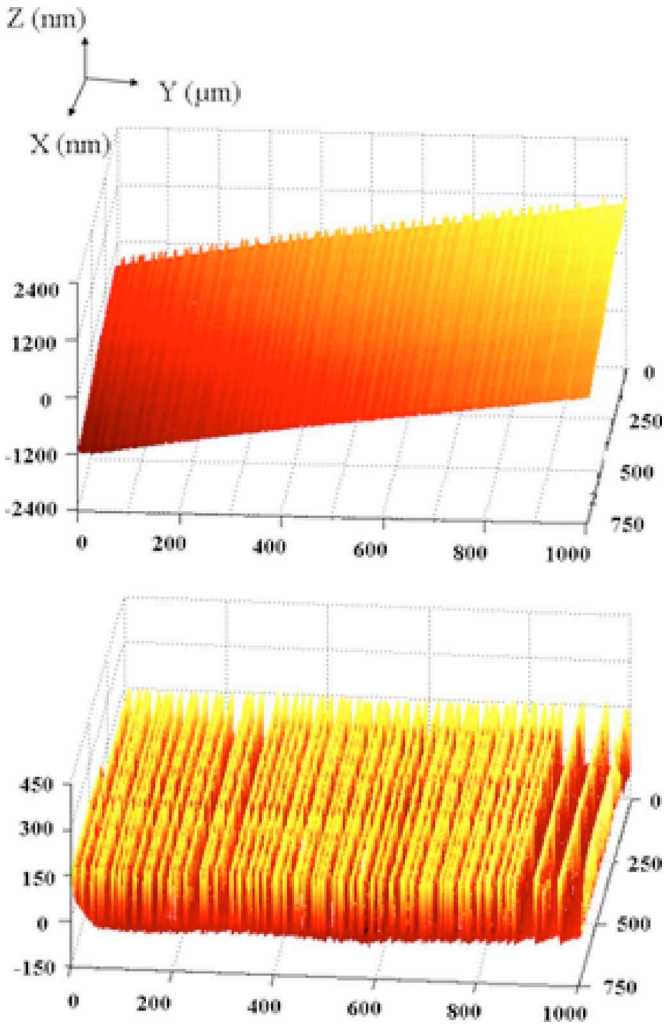

FIG. 3. (Color online) Long topographic image. This image is 750 nm wide (X axis) and 1 mm long (Y axis). The resolutions are 25 nm for the X axis (29 lines) and 20 nm for Y axis (50 000 points). The Z axis is the acquisition of the AFM signal. The entire image was achieved in about 25 min at a scan speed of 40 μm s^{-1}. The upper part is presented without any treatment. We can see shading-off colors due to remaining tilts in X and Y axes; the waveguides are rather difficult to detect. The lower part is the same image after background adjustment; waveguide structures appear along X axis. The image reveals that on this sample, the structures are parallel but irregularly spaced (according to the design pattern).

origins. These include a vertical tilt between the translation stage and the sample, an eventual thermal drift along the z axis,[10] in addition to a slight curved discrepancy due to either flatness defects of the SHU and the radius of curvature of the SOI sample. The waveguide structures seem distorted but this is still an artifact. One can note that the pedestals are asymmetrical. This artifact is due to scanning at a very high lateral speed of 40 μm/s. It can be eliminated by the use of a convenient tip in addition to subtracting the effect of abrupt tip-sample interactions.

Figure 5 shows a zoom revealing a single structure at the Y position of 217 μm. The upper part presents a 3D view in order to show a waveguide profile, while the lower part presents a cross section which allows appropriate measurements. With this zoom, the waveguide structure is not distorted anymore. The height and the width are compatible with those expected.

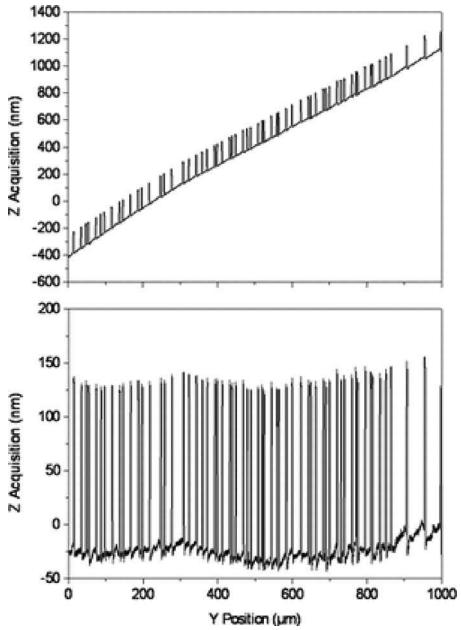

FIG. 4. Cross section of Fig. 3 along the *Y* axis. The upper part is presented without any treatment and points out the residual tilt. On the lower part, a third order polynomial fit was calculated and subtracted. The tilt that was subtracted corresponds to several cumulated effects: mainly the residual tilt but also the radius of curvature of the silicon substrate, slight flatness defects of the translation stages, and a probable thermal drift. Discrepancies at the base of the waveguide structure are artifacts due to the tip shape.

It is important to note that this zoom was obtained directly from the original image, while with a conventional AFM system, it would have been necessary to scan once again. The resolution is good enough to have a good representation of the parameters of both the macro- and nanostructures. With the millimeter large image of Fig. 3, a lot of waveguides are included. It is hence possible to check out the homogeneity at the chip level by means of statistical measurements.

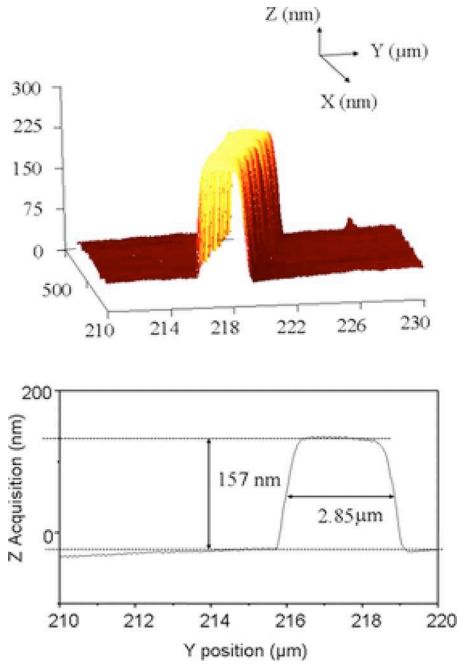

FIG. 5. (Color online) Zoom of one of the waveguide structure. It is obtained directly from the first image without scanning once again. The upper part presents a 3D view in order to show the waveguide profile, and the lower part presents a cross section which allows proper measurements. The figure illustrates one waveguide but statistics could be done over a set of structures.

C. Discussions

The herein reported millimeter scale atomic force microscopy image was obtained by 1 mm single scans repeated 29 times with a 25 nm spacing. Although accurate in only one dimension, the line-per-line mode was used. This first result demonstrates the feasibility of large displacements while addressing the constraints related to two-dimensional (2D) large scale imaging. The LL mode allows, in fact, us to scope large areas easily and quickly. However, results showed the expected layout of the structure that was scanned. No *XY* drift was noticed all along the surface. Accuracy in the *z* direction is left to the AFM and depends on the sensitivity of the sensors the AFM uses. In this experiment, a quadquadrant photodetector associated with an optical lever arm scheme was used. To meet higher performances, the SHU will have to be endowed with a traceable measurement along the *z* axis. This can be obtained by integrating a third laser interferometer within the SHU system.

Moreover, environmental condition supervision is critical to prevent any drift on the resulting image. For the SHU measurements to be more accurate, drift supervision and control shall be incorporated.[10] Refractive index measurements of the ambient air can also be taken into account with Édlen formula[31] to improve the positioning accuracy.

In addition to this, we plan in future works to extend the imaging area covered by the SHU especially in the short scan direction and to demonstrate the performances of the different scanning methods previously described.

Finally, the reported results only concern topographical characterization. With the same kind of setup, additional information can potentially be retrieved. We are currently working on the integration of the SHU to a combined atomic force-scanning near-field optical microscope.[2] Further works will also include adapting the SHU to ultimate applications such as lithography using a scanning electron microscope (SEM). The SEM is, in fact, very constraining since it requires very high speeds, temperature stabilization in addition to operating in vacuum. For this, reducing the SHU volume is currently under study.

ACKNOWLEDGMENTS

The authors are grateful toward E. Oseret from the Laboratoire de Parallélisme, Réseaux, Systèmes, et Modélisation (PRiSM) for his useful discussions about handling high density images. This project is cofunded by the French Government (ACI Nanosciences) and by the Ile-de-France region.

[1] The International Technology Roadmap for Semiconductors, Metrology report, 2005, http://www.itrs.net/Common/2005ITRS/Metrology2005.pdf
[2] R. Bachelot, G. Lerondel, S. Blaize, S. Aubert, A. Bruyant, and P. Royer, Microsc. Res. Tech. **64**, 441 (2004).
[3] S. Blaise, S. Aubert, A. Bruyant, R. Bachelot, G. Lerondel, P. Royer, J. E. Broquin, and V. Minier, J. Microsc. **209**, 588 (2003).
[4] S. C. Minne, J. D. Adams, G. Yaralioglu, S. R. Manalis, A. Atalar, and C.

F. Quate, Appl. Phys. Lett. **73**, 1742 (1998).
[5] H. Liu, B. Lu, Y. Ding, Y. Tang, and D. Li, J. Micromech. Microeng. **13**, 295 (2003).
[6] J. Fu, R. D. Young, and T. V. Vorburger, Rev. Sci. Instrum. **63**, 2200 (1992).
[7] H.-C. Yeh, W.-T. Ni, and S.-S. Pan, Control Eng. Pract. **13**, 559 (2005).
[8] M. Holmes, R. Hocken, and D. Trumper, Precis. Eng. **24**, 191 (2000).
[9] J. A. Kramar, Meas. Sci. Technol. **16**, 2121 (2005).
[10] G. Wilkening and L. Koenders, *Nanoscale Calibration Standards and Methods*, (Wiley-VCH, New York, 2005).
[11] F. Meli and R. Thalmann, Meas. Sci. Technol. **9**, 1087 (1998).
[12] J. Haycocks and K. Jackson, Precis. Eng. **29**, 168 (2005).
[13] R. Leach, J. Haycocks, K. Jackson, A. Lewis, S. Oldfield, and A. Yaccot, Nanotechnology **12**, R1 (2001).
[14] S. Ducourtieux, S. Duhem, F. Larsonnier, J. Salgado, G. P. Vailleau, L. Lahousse, and J. David, in Proceedings of the 5th Euspen International Conference, Montpellier, France, (2005) Vol. 1, pp. 131–134 .
[15] C.-W. Lee and S.-W. Kim, Precis. Eng. **21**, 113 (1997).
[16] J. Schneir, T. H. McWaid, J. Alexander, and B. P. Wilfley, J. Vac. Sci. Technol. B **12**, 3561 (1994).
[17] M. Bienias, S. Gao, K. Hasche, R. Seemann, and K. Thiele, Appl. Phys. A: Mater. Sci. Process. **66**, 837 (1998).
[18] G. B. Picotto and M. Pisani, Ultramicroscopy **86**, 247 (2001).
[19] S. Gonda, T. Doi, T. Kurosawa, Y. Tanimura, N. Hisata, T. Yamagishi, H. Fujimoto, and H. Yukawa, Rev. Sci. Instrum. **70**, 3362 (1999).
[20] J. Haycocks and K. Jackson, in Proceedings of the 2nd Euspen Conference, Torino, Italy, 2001, p. 392.
[21] K. R. Koops and K. Dirscherl, in Proceedings of 3rd Euspen Conference, Eindhoven, The Netherlands, 2002 , pp. 525–528.
[22] W. Gao, Y. Arai, A. Shibuya, S. Kiyono, and C. H. Park, Precis. Eng. **30**, 96 (2006).
[23] S. Topçu, L. Chassagne, D. Haddad, Y. Alayli, and P. Juncar, Rev. Sci. Instrum. **74**, 4876 (2003).
[24] S. Topçu, L. Chassagne, Y. Alayli, and P. Juncar, Opt. Commun. **247**, 133 (2005).
[25] L. Chassagne, S. Topcu, Y. Alayli, and P. Juncar, Meas. Sci. Technol. **16**, 1771 (2005).
[26] K. Dirscherl, Ph.D. thesis, Technical University of Denmark, Lyngby, 2000.
[27] C.-L. Hwang, Y.-M. Chen, and C. Jan, IEEE Trans. Control Syst. Technol. **13**, 56 (2005).
[28] N. Bobroff, Precis. Eng. **15**, 33 (1993).
[29] F. C. Demarest, Meas. Sci. Technol. **9**, 1024 (1998).
[30] Pacific Nanotechnology Inc., Nano-R atomic force microscope specifications, http://www.pacificnanotech.com/nano-r-spm.html
[31] K. P. Birch and M. J. Downs, Metrologia **30**, 155 (1993).